Fas receptor induces apoptosis of synovial bone and cartilage progenitor populations and promotes bone loss in antigen-induced arthritis

Running title: Fas and osteoprogenitors in arthritis

Elvira Lazić Mosler*[1,4,5], Nina Lukač*[1,2], Darja Flegar[1,3], Martina Fadljević[1], Igor Radanović[1], Hrvoje Cvija[1], Tomislav Kelava[1,3], Sanja Ivčević[1,6], Alan Šućur[1,3], Antonio Markotić[1,7], Vedran Katavić[1,2], Ana Marušić[8], Danka Grčević[1,3], Nataša Kovačić[1,2]

**equal first authors*

Affiliations:

[1]Laboratory for Molecular Immunology, Croatian Institute for Brain Research, University of Zagreb School of Medicine, Šalata 12, Zagreb, Croatia

[2]Department of Anatomy, University of Zagreb School of Medicine, Šalata 11, Zagreb, Croatia

[3]Department of Physiology and Immunology, University of Zagreb School of Medicine, Šalata 3, Zagreb, Croatia

[4]General Hospital Dr. Ivo Pedišić, JJ Strossmayera 59, Sisak, Croatia

[5]Catholic University of Croatia, Ilica 242, Zagreb, Croatia

[6]Huntsman Cancer Institute, University of Utah, Salt Lake City, USA

[7]Centre for Clinical Pharmacology, University Clinical Hospital Mostar, Mostar, Bosnia and Herzegovina

[8]Department of Research in Biomedicine and Health, University of Split School of Medicine, Šoltanska 2, Split, Croatia

Corresponding author:

Nataša Kovačić, MD, PhD

Department of Anatomy

University of Zagreb School of Medicine

Šalata 11, HR-10000 Zagreb, Croatia

E-mail: natasa.kovacic@mef.hr

Telephone and fax nuber: ++385 1 4566 846 / ++385 1 4590 195

List of nonstandard abbreviations

AIA – antigen-induced arthritis

AF488 – Alexa Fluor 488

APC – allophycocyanin

ACPCy7 – APC-cyanine 7

bglap - bone gamma-carboxyglutamate (gla) protein, osteocalcin gene

BV/TV – trabecular bone volume

CFA – complete Freund's adjuvant

ColIα2 – collagen type 1, α2 chain gene

DAPI – 4',6-diamidino-2-phenylindole dihydrochloride

Fas –/– – Fas knockout

FITC – fluorescin isothiocyanite

FLS – fibroblast-like synoviocyte

IL – interleukin

IFN – interferon

lpr – lymphoproliferative syndrome

mBSA – methylated bovine serum albumin

μCT – micro-computerized tomography

OPG – osteoprotegerin

PE – phycoerythrin

PECy7 – PE-cyanine 7

RA – rheumatoid arthritis

RANKL – receptor activator of nuclear factor κB ligand

Runx2 – runt-related transcription factor 2 gene

Tb.N – trabecular number

Tb.Th – trabecular thickness

Tb.Sp – trabecular separation

TNF – tumor necrosis factor

wt – wild-type

7-AAD – 7-aminoactinomycin D

Abstract

Rheumatoid arthritis is inflammatory joint disease which eventually leads to permanent bone and cartilage destruction. Fas has already been established as the regulator of inflammation in RA, but its role in bone formation under arthritic conditions is not completely defined.

The aim of this study is to assess the effect of Fas inactivation on the bone damage during murine antigen-induced arthritis (AIA). Subchondral bone of wild-type (wt) and Fas-knockout (Fas –/–) mice was evaluated by histomorphometry and micro-computerized tomography. Proportions of synovial bone and cartilage progenitors were assessed by flow cytometry. Synovial bone and cartilage progenitors were purified by FACS-sorting and expression of Fas and Fas-induced apoptosis were analyzed *in vitro*.

Results show that Fas –/– mice develop attenuated arthritis characterized by preserved epiphyseal bone and cartilage. A proportion of earliest $CD200^+$ bone and cartilage progenitors is reduced in wt mice with arthritis, and unaltered in Fas –/– mice. During osteoblastic differentiation *in vitro*, $CD200^+$ cells express highest levels of Fas and are removed by Fas ligation.

These results suggest that Fas-induced apoptosis of early $CD200^+$ osteoprogenitor population represents potential mechanism underlying the impaired bone formation in arthritis, so their preservation may represent the bone protective mechanism during arthritis.

Keywords: mesenchymal cells, osteoprogenitors, osteoblasts, rheumatoid arthritis

Introduction

Rheumatoid arthritis (RA) is a systemic autoimmune disease characterized by a symmetric polyarthritis, which eventually results in permanent disability due to destruction of articular cartilage and underlying bone. The main characteristic of RA is synovial thickening resulting from uncontrolled fibroblast-like synoviocyte (FLS) proliferation, accompanied by infiltration of synovium by lymphocytes, macrophages and neutrophils (1). Infiltrating cells, as well as proliferating FLS produce pro-inflammatory cytokines, such as tumor necrosis factor (TNF), interleukin (IL)-1, -6, -7, -8, -15, -17, -18, -32, -35, and interferons (IFN) (2–10). Beside their role in initiating and supporting inflammation, these cytokines also contribute to bone damage by affecting the balance between osteoclastic bone resorption and osteoblastic bone formation (11,12). Many of the mentioned cytokines affect homing and activation of osteoclast progenitors, or increase the expression of receptor activator of NF-κB ligand (RANKL) on osteoblastic and activated T cells, and thus, enhance osteoclastogenesis (12–14). Increased NFκB signaling triggered by inflammatory cytokines also reduces the differentiation potential of mesenchymal cells in the affected joints (15–17). In addition, the inflammatory milieu suppresses the Wnt-pathway, important for differentiation and function of osteoblasts (18).

Pathogenesis of arthritis is also influenced by survival and apoptosis of inflammatory and synovial cells. Apoptosis can be induced externally, by the ligation of death receptors from the TNF family, which are able to activate caspase signaling via the intracytoplasmic death domain (19). Fas (CD95, Apo-1), a typical death receptor, is a well characterized regulator of the immune system homeostasis, and ubiquitously expressed on different cells and tissues (20). Increasing evidence suggests the involvement of the Fas/Fas ligand system in bone homeostasis (21–25). As an immune regulator, the Fas/Fas ligand system has already been attributed to the pathogenesis of RA and other inflammatory arthritides, but there are contradicting reports on the beneficial, as well as detrimental roles in the pathogenic process (26,27). For instance, hyperplastic FLS and infiltrating cells express Fas, so administration of Fas agonistic antibody, or Fas ligand delivery ameliorated arthritis (28–30). However, hyperplastic FLS are resistant to apoptosis, due to expression of anti-apoptotic molecules, or inadequate contribution of the internal, mitochondrial apoptotic pathway (31,32). On the other hand, systemic inactivation of Fas in DBA/lpr strain alleviates murine collagen-induced arthritis due to ineffective signaling through IL-1R in macrophages (33,34). A recent study also showed faster resolution of K/BxN murine arthritis, in mice with a conditional depletion of Fas in myeloid cells due to the reduced expression of toll-like receptor (TLR) ligand gp96 and enhanced expression of IL-10 in macrophages (35).

In this study, we report on the attenuated form of antigen-induced arthritis (AIA) in Fas-deficient (Fas –/–) mice and address the potential role of Fas in the regulation of local bone formation under the arthritic conditions by controlling synovial bone and cartilage progenitor apoptosis and differentiation.

Materials and methods

Mice

Eight to twelve-week old female C57BL/6J wild-type (wt) mice and mice deficient in the Fas gene (Fas −/−) on the C57BL/6 background (36) were used in all experiments. The Fas −/− mice and corresponding wt control (C57BL/6J) strain were a gift from Dr. M. Simon (Max Planck Institute for Immunobiology, Freiburg, Germany). Both colonies were bred and maintained at the animal facility of the Croatian Institute for Brain Research, University of Zagreb, School of Medicine, under standard conditions (10 hours light and 14 hours dark daily, standard chow (4RR21/25; Mucedola, Italy) and water *ad libitum*). All animal protocols were approved by the Ethics Committee of the University of Zagreb, School of Medicine (380-59-10106-15-168/235) and the National ethics committee (EP 07-2/2015), and conducted in accordance with accepted standards of ethical care and use of laboratory animals.

Antigen-induced arthritis (AIA)

Mice were immunized with 200 μg methylated bovine serum albumin (mBSA, Sigma-Aldrich, St Louis, MO, USA) emulsified in 0.2 ml complete Freund's adjuvant (CFA, Sigma-Aldrich) injected subcutaneously into the flank skin (9). Seven days after the first injection, the mice were injected intradermally with 100 μg mBSA in 0.1 ml CFA at the base of the tail. Arthritis was induced on day 21 by intra-articular (i.a.) injection of 50 μg mBSA dissolved in 10 μl sterile phosphate buffered saline (PBS) into both knees, under tribromoethanol (Sigma-Aldrich) anesthesia. Controls were injected i.a. with 10 μl of sterile PBS. Mice were sacrificed on day 31 (day 10 post-i.a. injection) by cervical dislocation under tribromoethanol anesthesia. After skin removal, transverse diameters of knee joints were measured 3 times for each knee by a vernier scale/caliper. Right knees were harvested for histological assessment of arthritis, histomorphometry or micro-computerized tomography (μCT), and left knees for flow cytometry, cell sorting, and osteoblastogenic cultures.

Histological assessment of arthritis

Knee joints were dissected, released from soft tissues, and fixed in 4% formaldehyde at 4°C for 24 hours. Fixed tissues were decalcified for 2 weeks in 14% ethylene-diamine tetra-acetic acid and 3% formalin, dehydrated in increasing ethanol concentrations, and embedded in paraffin. Six μm sections were cut with a Leica SM 2000 R rotational microtome (Leica, Nussloch, Germany). Histological assessment was performed on the frontal sections (6 μm) through the knee joint stained with Goldner-trichrome or toluidine blue. Histological sections were scored semi-quantitatively in a blinded fashion (by concealing labels and random assignment of numbers before scoring) for the following parameters of joint destruction: synovitis, joint space exudate, cartilage degradation and subchondral bone damage using a 0-3 point scale (37). A combined arthritis score was generated as the sum of scores for the above 4 parameters (maximum score 12).

Histomorphometry

Histomorphometry was performed in a blinded fashion using Axio Imager microscope (Carl Zeiss Inc, Oberkochen, Germany) equipped with a charge-coupled device (CCD) camera connected to a computer with appropriate software (OsteoMeasure, Osteometrics, Decatur, GA, USA).

Histomorphometric analysis was performed under 100× magnification, in 4 Goldner-trichrome- and toluidine blue-stained distal frontal femoral sections, taken from 4 corresponding depths for each specimen, measuring separately mineralized trabeculae in distal mid-epiphyseal region. Analyzed variables were automatically calculated by the OsteoMeasure software and included trabecular bone volume (BV/TV, %), trabecular number (Tb.N, mm^{-2}), trabecular thickness (Tb.Th, μm), and trabecular separation (Tb.Sp, mm).

Micro-computerized tomography

The distal femora were scanned using a μCT system (1076 SkyScan, Bruker, Kontich, Belgium), at 50kV and 200 μA with a 0.5 aluminum filter. Detection pixel size was 9 μm, and images were captured every 0.4° through 180° rotation of the camera. The scanned images were reconstructed using the Recon software (SkyScan) and analyzed using the CTAn software (SkyScan). Three-dimensional analysis and reconstruction of the epiphyseal trabecular bone was performed on transverse sections in the region beginning above the epiphyseal line (excluding the dense zones adjacent to the epiphyseal cartilage) and ending at the level of separation of the condyles. Measured variables were trabecular bone volume (BV/TV, %), trabecular number (Tb.N, mm^{-2}), trabecular thickness (Tb.Th, μm), and trabecular separation (Tb.Sp, mm).

Flow cytometry and cell sorting

Tibiae and femora were cut at the level of the growth plates, the isolated joints cleaned from the surrounding soft tissues, injected with 1 mg/ml collagenase type IV (Sigma) and incubated for 1 h at 37 °C to release synovial cells. Cultured synovial cells were dissociated from the surface by TrypLE Express (Thermo Fisher). Single cell suspensions were prepared by passing the cells through a 100 μm-cell strainer, and suspensions containing $2\text{-}5\times10^6$ cells were transferred to FACS tubes. Non-specific antibody binding was blocked by adding 0.5 μl of anti-mouse CD16/CD32 (eBiosciences, 93) per sample and incubating for 5 min at RT. After blocking, cells were stained with the 6-colour panels using the following antibodies: anti-CD95-AF488 (eBiosciences, 15A7) and/or anti-CD95-FITC (BD Biosciences, Jo2), or corresponding isotype controls (mouse IgG1κ-AF488, eBiosciences, armenian hamster IgG2λ-FITC, BD Biosciences), CD45-APC (eBiosciences, 30-F11), CD31-PECy7 or APC (eBiosciences, 390), TER119-PE or APC (eBiosciences, TER119), CD51-biotin (BioLegend, RMV-7), CD200–PE (eBiosciences, OX90), CD105-PECy7 (eBiosciences, MJ7/18), CD90.2-FITC (eBiosciences, 30-H12), Sca-1-FITC (eBiosciences, D7), CD140b-PECy7 (eBiosciences, APB5), CD11b-PE (eBiosciences, M1/70), Gr-1-PECy7 (eBiosciences, RB6-8C5), B220-APC (eBiosciences, RA3-6B2), and CD3-APCCy7 (eBiosciences, 145-2C11) antibodies. Dead cells were excluded by binding of 7-amino-actinomycin D (7-AAD, BioLegend) or propidium iodide (PI, Thermo Fisher Scientific, Waltham, Massachusetts, USA). After

incubation for 30 min at 4°C, cells were washed with PBS and incubated with streptavidin-APCeFluor780 (eBiosciences, Thermo Fisher Scientific) for the following 30 min at 4°C, washed, resuspended in PBS containing 10 μl of 7-AAD per mL, acquired on Attune (Thermo Fisher Scientific) instrument and analysed by FlowJo software (FlowJo, Ashland, OR, USA). Annexin V (BioLegend, San Diego, California, USA) and 7-AAD staining were performed according to the manufacturer's instructions.

Cell sorting was performed by a BD FACSAria I (BD Biosciences, Franklin Lakes, New Jersey, USA) instrument, as described previously (38). Labelled cells were acquired at a speed 2000-5000 cells/s using the following gating strategy: singlets were delineated from total cell population depicted on forward- versus side-scatter plot, exclusion of dead cells was based on 4',6-diamidino-2-phenylindole dihydrochloride (DAPI, Sigma-Aldrich) incorporation, and subsequent dissection of populations of interest. Defined populations of hematopoietic and stromal cells were sorted in 2 ml collection tubes containing PBS with 2% FCS and used for cell cultures. Sorting parameters were optimized for high purity sorting. Sorting purity was determined by a re-analysis of fractioned populations and was greater than 99% for all experiments.

Cell culture

Cells were plated in 6- or 24-well culture plates at a density of 2.5×10^5 cells in 0.35 ml of α-MEM per cm^2 surface for primary cultures, and 1.5×10^4 cells in 0.35 ml of α-MEM per cm^2 surface for sorted mesenchymal cell cultures, supplemented with 10% FCS (Gibco, Thermo Fisher Scientific). Osteoblast differentiation was induced by the addition of 50 μg/mL ascorbic acid, 10^{-8} M dexamethasone and 8 mM β-glycerophosphate. Osteoblast colonies were identified histochemically by the activity of alkaline phosphatase (AP), using a commercially available kit (Sigma-Aldrich). Red stained ALP+ osteoblast surface per well was measured by a custom-made software (39). Mineralisation was estimated by alizarin red (Sigma-Aldrich) staining and semi-quantified by acetic acid mediated extraction of dye and spectrophotometry (40). Total colonies were stained with methylene blue (MB).

Induction of apoptosis

For the induction of apoptosis, 1 μg/mL of anti-mouse CD95 antibody (BD Biosciences, clone Jo2) or the corresponding isotype control (armenian hamster IgG2λ, BD Biosciences) and 1 μg/mL protein G (Sigma-Aldrich) were added to osteoblastogenic cultures on days 6 and 13, and incubated for 16-18 h. Cells treated only with 1 μg/mL protein G were used as non-treated controls.

Gene expression analysis

Total RNA was extracted using a TRIzol reagent (Thermo Fisher Scientific). For PCR amplification, total RNA was converted to cDNA by reverse transcriptase (Thermo Fisher Scientific), and amplified by an ABI 7500 instrument (Applied Biosystems, Thermo Fisher Scientific), using commercially available TaqMan Assays (mouse Fas, Mm00487425_m1; mouse FasL, Mm00438864_m1; mouse TNF, Mm00443258_m1; mouse IL1-

β, Mm00434228_m1; mouse RANKL, Mm00441906_m1; mouse OPG, Mm00435452_m1; mouse IL-6, Mm00446190_m1; mouse IL-10, Mm01288386_m1; mouse β-actin, Mm00607939_s1; mouse Runx2, Mm00501584_m1; mouse ColIa2, Mm00483888190_m1; mouse osteocalcin, Mm03413826_mH Thermo Fisher), as described previously (21).

Data analysis and interpretation

Data are plotted as individual values, horizontal lines and markers represent means±SD or medians±IQR. Statistical analysis has been performed by MedCalc Statistical Software version 12.5.0 (MedCalc Software bvba, Ostend, Belgium). Depending on the number of factors, distribution and type of variables, data were analyzed by two-way ANOVA or one-way ANOVA with Student-Newman-Keuls post hoc test, or Kruskal-Wallis test with pairwise comparisons according to Conover (41).

Results

Functional Fas receptor is required for development of destructive AIA

To assess the effects of Fas inactivation on the severity of AIA, we first analyzed joint swelling, histological signs of joint destruction, and characteristics of epiphyseal trabecular bone (Fig 1A). Ten days post-i.a. injection, the transverse diameters of knee joints were greater in wt mice with AIA compared to the wt control group (Fig 1B), and such increase was absent in Fas –/– mice (Fig 1B). The summary histology score was significantly higher in both groups of mice with arthritis, in comparison to respective controls (Fig 1C). Analysis of individual scored elements showed that mild synovitis and exudate occasionally develop in arthritic Fas −/− mice, whereas bone and cartilage destruction were even less common in contrast to arthritic wt mice (Fig 1E). A superficial zone of degraded cartilage was a common finding in wt mice with arthritis, but extremely rare in any of the other groups. Quantitatively assessed, percentage of non-degraded cartilage in the total cartilage thickness was significantly lower in wt mice with arthritis (Fig 1D). In Fas −/− mice, both, the control group and mice with arthritis, we observed only non-degraded cartilage (Fig 1D).

Assessed by both, histomorphometry and micro-CT, distal femoral epiphyseal trabecular bone volume and trabecular thickness responded differently to arthritis in Fas –/– mice than in wt controls. Both variables were decreased in wt mice with AIA in comparison to the control group, and similar in both groups of Fas –/– mice (Fig 2A and C). Micro-CT analysis showed irregularities and multiple erosions on the epiphyseal subchondral bone plate in wt AIA, which were absent in Fas –/– mice (Fig 2B). In addition, micro CT revealed different response of trabecular number in Fas –/– mice with arthritis, characterized by lower trabecular number in wt mice with AIA and similar in Fas –/– mice with AIA, in comparison to their respective controls (Fig 2C).

Fas expression is upregulated in AIA in hematopoietic and non hematopoietic cells

To determine the populations potentially regulated by Fas in AIA, we analyzed the surface expression of Fas on hematopoietic ($CD45^+TER119^+$) and endothelial ($CD31^+$) vs. non hematopoietic ($CD45^-TER119^-CD31^-$) cells in the joints from mice with arthritis and control mice. We expected that immunization itself would affect the expression of Fas due to the activation of cells of the immune system, so we also analyzed cells from the non immunized mice in addition to immunized control and arthritic mice, in order to distinguish the effect of immunization from the effect of local inflammation after arthritis induction. The systemic effect was further assessed by analyzing Fas expression on the splenocyte subsets in all three experimental groups.

Flow cytometry analysis showed a significant increase in the surface expression of Fas on the total population of synovia-derived cells in control immunized mice groups, in comparison to control non immunized group. In mice with arthritis, expression was lower than in control immunized mice, but still significantly higher than in control non immunized group (Fig 3A, upper left panel). The same pattern of expression was observed on the hematopoietic and non hematopoietic populations (Fig 3A, upper panels). The pattern of expression of

separately analyzed hematopoietic CD45, CD31 and TER119 synovia-derived populations was similar (Fig 3A, middle panels). On the systemic level, assessed by analyzing splenocyte subsets, expression pattern on T cells was similar to synovia-derived populations, and characterized by increased expression of Fas as a result of immunization, followed by a decrease in Fas upon induction of arthritis. Expression of Fas on myeloid ($CD11b^{+}Gr1^{+}$) splenocyte population was not different between immunized and non immunized controls, and downregulated in mice with arthritis. Expression of Fas on splenic B cells was similar in both immunized groups, and slightly higher than in non immunized mice (Fig 3A, lower panels). Taken together, this reveals both, immune and osteoprogenitor populations, as potential cellular targets of Fas/Fas ligand system in arthritis. To assess the overall regulation of Fas/Fas ligand system, in the context of inflammatory activity and bone remodeling, we analyzed the expression of selected genes in total joint tissue extracts from wt and Fas –/– mice with arthritis, and compared them with baseline expression in non immunized mice. On day 10 post-induction of arthritis, Fas expression was more than 2-fold up-regulated only in three out of five samples from wt mice in comparison to non immunized controls, so the overall increase was not significant (Fig 3B, upper panels). This was potentially a result of assessment at day 10, when inflammatory activity is ceasing. In early acute arthritis (day 3 post-induction) we detected 2-5-fold increase in all samples of wt mice with arthritis in comparison to NI controls ($p=0.005$, N=4, Kruskal-Wallis test, not shown) pointing to the transcriptional up-regulation in early arthritis. The expression of Fas ligand was similar in all groups of mice (Fig 3B, upper panels). Major pro-inflammatory cytokines TNF, IL-1β, and IL-6 (Fig 3B, upper right and middle panels) was, as expected, higher in wt mice with arthritis than in non immunized wt mice. The levels of IL-1β and IL-6, as well as of anti-inflammatory IL-10 were also significantly higher in wt mice with AIA in comparison to Fas –/– mice with AIA, whereas levels of TNF were comparable between both groups of mice with arthritis. This overall cytokine profile points to a conclusion that inflammation is less extensive in the joints of Fas −/− mice with AIA, which is further in line with the results of histology scoring, but contrasts the previously described findings in *lpr* mice with collagen-induced arthritis (33). Absence of bone loss in Fas –/– mice was reflected in the expression of RANKL and OPG as important regulators of bone remodeling. Joints from wt mice with arthritis expressed significantly more pro-osteoclastogenic RANKL than non immunized wt mice, while the levels were lower in Fas –/– with arthritis in comparison their non immunized control, as well as in comparison to wt AIA group. At the same time, expression of anti-osteoclastogenic osteoprotegerin (OPG) was decreased in wt mice with AIA in comparison to non-immunized control and Fas –/– mice with AIA, and similar in both Fas –/– groups (Fig 3B, lower panels). RANKL/OPG ratio was thus, increased in wt mice with AIA, similar in both groups of Fas –/– mice, and significantly lower in Fas –/– mice with AIA in comparison to wt AIA group, confirming the bone-preserving effect of Fas deficiency in the subacute phase of AIA documented by histology and histomorphometry (Fig 3B, lower right panel).

Synovial subpopulations of bone and cartilage progenitors are differentially regulated in Fas-deficient mice with arthritis

Upregulation of Fas in arthritis, and alterations in inflammatory cytokine expression, point to a role of Fas in the regulation of many aspects of joint inflammation, which could directly or indirectly induce misbalanced bone remodeling and result in permanent joint damage. Suppressed inflammation, and decreased RANKL/OPG ratio in Fas –/– mice with arthritis points to the requirement of Fas to support inflammation and enhance osteoclastogenesis. However, as we previously described effects of Fas on osteoblast maturation and apoptosis (21), we hypothesized that bone-sparing effect of Fas inactivation might also be mediated through non hematopoietic population containing bone and cartilage progenitors. Beside its role in reparative processes, this population is also the source of OPG, whose expression was altered by Fas deficiency.

We first assessed the osteoblast differentiation from total synovial cells. Cells were harvested on day 10 post i.a. injection, and the surface covered with AP positive colonies was measured after 14 days of cell culture. To confirm osteoblastogenic differentiation, we determined the expression of osteoblast-specific genes runt-related transcription factor 2 (*Runx2*) collagen type I, α2 chain (*ColIα2*), osteocalcin (*bglap*), and osteoprotegerin (*OPG*), over the culture course. Osteoblastogenesis was not significantly affected by arthritis in both groups of mice, which was reflected by lack of significant effect of Fas deficiency or arthritis on the surface covered by ALP+ osteoblast colonies, as well as on the expression of osteoblast genes (Fig 4 A-C). Ex vivo culture conditions reflect the number and differentiation potential of mesenchymal cells, but not necessarily their differentiation within the inflammatory microenvironment, so we further focused on the analysis of proportions of resident subpopulations of non hematopoietic synovial cells ($CD51^+CD45^-TER119^-CD31^-$), and among them, proportions of cells bearing various mesenchymal and osteoblast markers, such as Sca-1, CD140b, CD44, and a modified set of osteoprogenitor markers recently characterized by Chan et al (42). According to Chan et al., osteoprogenitors are contained among the population of $CD51^+CD45^-TER119^-CD31^-$ cells, and were further separated according to the expression of CD200, CD90.2 and CD105. $CD51^+CD200^+$ cells correspond to the earliest progenitors (skeletal stem cells, SSC), whereas $CD51^+CD200–$ cells are committed progenitors (Fig 4D). Further osteogenic/chondrogenic differentiation results in acquisition of CD105 and CD90.2 markers. Committed cartilage progenitors co-express CD200 and CD105, so we considered $CD200^+CD105^-$ as SSCs. The proportion of total non hematopoietic $CD51^+CD45^-TER119^-CD31^-$ population was not affected by arthritis or Fas inactivation (Fig 4E), and proportions of $CD140b^+$, $Sca\text{-}1^+$ and $CD44^+$ cells had no consistent pattern among experiments (not shown). In wt mice with arthritis, the proportion of $CD51^+CD200^+$ cells (SSC) was lower in comparison to control mice, and accompanied by a corresponding increase in the proportion of $CD51^+CD200^–$ cells, while the ratio between both populations was similar in control and AIA groups of Fas −/– mice (Fig 4E). The frequency of cells corresponding to committed bone progenitors ($CD51^+CD200–$

$CD105^{+}CD90.2^{+}$) was not altered by arthritis, but higher frequencies were observed in Fas −/− mice pointing to changed differentiation kinetics by the state of Fas deficiency (Fig 4E).

Synovial bone and cartilage progenitors express Fas and have a different susceptibility to Fas-mediated apoptosis

To confirm the functional role of Fas receptor on synovia-derived bone and cartilage progenitors, we assessed the expression and function of Fas during osteoblastogenic differentiation of mesenchymal progenitors from the synovial compartment. To establish pure primary mesenchymal population, we FACS-sorted $CD45^{-}CD31^{-}TER19^{-}CD51^{+}$ cells, and expanded them *in vitro*. Flow cytometry analysis confirmed the absence of hematopoietic or endothelial markers, high expression of CD51, substantial expression of CD200, and variable expression of CD105 (Fig 5A-B). Osteoblast differentiation *in vitro* was marked by an increase in proportion of $CD200^{+}$ cells, and corresponding decrease in $CD200^{–}$ cells (Fig 5A-B). In osteoblastogenic cultures, 80-90% cells expressed Fas on a culture day 7, with decrease to 50-70% towards day 14, and corresponding results on the transcriptional level (Fig 5C-E). Expression of Fas was lower on CD200– cells, with prominent decrease towards day 14 in comparison to $CD200^{+}$ cells (Fig 5C, D). Synovial progenitors were capable of forming AP positive colonies on both, days 7 and 14 and, later in the culture course (day 14), alizarin red-stained mineralized nodules (Fig 5 F,G).

To establish the function of Fas receptor expressed on mesenchymal progenitors, we treated these cultures with anti-Fas antibody on days 6 and 13, which resulted in a substantial increase in the numbers of apoptotic and dead cells on day 7 and 14 (Fig 6A). Sixteen hours after Fas treatment there was a reduction in proportion of $CD200^{+}$ cells in both time points of osteoblastogenic cultures (Fig 6B), confirming that $CD200^{+}$ cells are susceptible to Fas-induced apoptosis.

Discussion

This study reveals an important role of Fas receptor in development of destructive form of murine AIA, not only by supporting inflammation, but also by inducing osteoprogenitor apotosis and thus, affecting bone formation. Clinical and histological scoring showed a particular absence of cartilage and bone destruction in Fas-deficient mice with AIA, with an occasional presence of mild inflammation. In addition to the absence of subchondral bone erosions, the loss of epiphyseal trabecular bone and thinning of the epiphyseal trabeculae were absent in Fas –/– mice, in comparison to the wt mice with arthritis, which is in accordance with our previous findings on positive effects of the Fas/Fas ligand system deficiency on bone mass (23,43). In this report, we quantified the subchondral epiphyseal trabecular bone with the aim to assess the bone damage associated specifically with local inflammation, rather than standard quantification of metaphyseal bone, which might also reflect the existence of systemic inflammation-induced osteopenia.

Our findings are consistent with previous studies documenting attenuated murine collagen-induced arthritis (CIA), and a faster resolution of a chronic phase of K/BxN arthritis in murine models of Fas inactivation (33-35). These results were ascribed to altered pro-inflammatory signaling through IL-1R, and revealed Fas signaling in macrophages as an important regulator of the inflammatory process (33-35). Opposite to these studies, who report similar or increased levels of proinflammatory cytokines in joints of Fas-deficient mice in comparison to controls, on protein or transcriptional level, we found decreased levels of major proinflammatory cytokines IL-1β and IL-6 in Fas –/– mice with AIA. This might reflect the different experimental models of arthritis or mouse strain used in the above mentioned studies. *lpr* mice used in studies by Tu Rapp et al., and Ma et al. are described to have a leaky spontaneous mutation which may account for differences in the pathogenic mechanism (33,34,36). In addition, these discrepancies could be time-point related. A detailed kinetic study of cytokine expression performed in rats revealed differences in cytokine expression over the course antigen–induced arthritis. TNF transcription peaks during first 24 hours after i.a. injection of antigen, and after that returns to basal levels, whereas IL-1β and in particular IL-6 pertain transcriptionally elevated over the period of two weeks (44). Therefore, our results on day 10 post-induction do not fully depict the complex changes of cytokine pattern over the disease course, but provide additional evidence for less extensive inflammation at that time point, already established by histology score. However, the crucial outcome assessed in our study was local bone damage which results in deformities and disability, and represents clinically important feature of RA, developing as a result of complex interactions between immune cells, as well as resident cell populations in the affected joints. Certain forms of autoimmune and inflammatory arthritides, such as the arthritis occurring in systemic lupus erythematosus (SLE), exert intensive soft tissue pathology marked by a presence of synovial infiltrate, edema and joint exudate, but without underlying bone destruction (45). Similarly, the phenotype of Fas-deficient C57B6 mice used in our study is characterized by lymphoproliferation and formation of

autoantibodies (46), corresponding to human SLE. Despite that, Fas-deficient mice are protected from joint inflammation and subsequent bone destruction. The ability of inducing apoptosis, as well as altering differentiation and activity of bone cells by the Fas/Fas ligand system has already been documented (21,22,25,47), and present study confirmed upregulation of Fas on the non hematopoietic population of cells within the arthritic synovial compartment. Upregulation of Fas protein on the cells of the immune system in the spleen and synovial compartment in response to immunization is an expected finding considering the well-known role of the Fas/ Fas ligand system in limiting the immune activation (48–50). As we have previously confirmed the regulatory effect of Fas on osteoblast lineage cells, and documented the decrease in RANKL/OPG ratio in Fas –/– mice with arthritis, we further focused on the analysis of the osteoprogenitor population, responsible for bone formation, as well as for counteracting inflammation-induced increase in osteoclast differentiation and activity. Although the osteoblastogenic potential, as well as the frequency of total non hematopoietic population containing mesenchymal progenitors were similar in synovial compartment of wt and Fas −/− mice with AIA, we observed differences in proportions of subpopulations of mesenchymal progenitors, which may implicate the specificities of a local microenvironmental control of osteoblast development and function. The proportion of $CD51^+CD200^+$ cells, corresponding to early bone and cartilage progenitors was decreased in wt mice with AIA, accompanied by an increase in the proportion of $CD51^+CD200–$ cells, corresponding to committed bone and cartilage progenitors (42). A decrease in the proportion of $CD51^+CD200^+$ population in wt mice with AIA, and an unaffected ratio of $CD51^+CD200–$/ $CD51^+CD200^+$ cells in Fas –/– mice with arthritis, may reflect the removal of $CD51^+CD200^+$ by Fas-mediated apoptosis, which in arthritis depletes the osteoprogenitor pool, and contributes to an ineffective bone formation. *In vitro*, osteoprogenitors were sensitive to Fas-induced apoptosis, with a more effective downregulation of Fas with progressing maturation, in $CD51^+CD200–$ population. A lower frequency of earliest $CD51^+CD200^+$ progenitor cells in Fas –/– mice in comparison to wt control group implies different kinetics of the bone progenitor differentiation, which is further reflected in increased proportion of committed bone progenitors, $CD51^+CD200–$ $CD90.2^+$ $CD105^+$ cells, and suggests a more robust bone formation potential. In addition, a recent study has shown that CD200 is required for the immunoregulatory capacity of mesenchymal cells, affecting differentiation of myeloid cells through its interaction with CD200R (51). Depletion of FasL-susceptible $CD200^+$ cells from synovial compartment, therefore, may contribute not only to the exhaustion of the osteoprogenitor pool, but also perpetuate inflammation and, in effect, favor the differentiation of myeloid lineage-derived osteoclasts.

In conclusion, the bone and cartilage progenitors in the synovial compartment represent a small but a highly adaptable population, so the preservation of the pool of the early osteoprogenitor subset in the state of Fas deficiency may represent the additional bone protective mechanism during AIA in Fas −/− mice. As Fas can

induce death of these cells, further understanding of this process might reveal potential new approaches to counteract local bone destruction during arthritis.

Acknowledgements

This work was supported by the grants No. 7406 and 5699, Scientific Center of Excellence for Reproductive and Regenerative Medicine (project "Reproductive and regenerative medicine - exploration of new platforms and potentials", Grant Agreement KK01.1.1.01.0008, funded by the European Union through the European Regional Development Fund), and Croatian Ministry of Science, Education and Sports Grant No. 1080229-0140.

We thank Laboratory for Mineralized Tissues, School of Medicine, University of Zagreb, for access to the 1076 SkyScan μCT instrument, Mrs Katerina Zrinski-Petrović for her technical assistance, and dr Ivan Krešimir Lukić for advising us regarding statistical analysis.

None of the authors has any conflict of interest regarding the submitted article.

Author Contributions

E. Lazić Mosler and N. Lukač designed research, performed research, analyzed data, and wrote the paper.

D. Flegar, M. Fadljević, I. Radanović, H. Cvija, T. Kelava, A. Markotić, S. Ivčević, and A. Šućur performed research and analyzed data.

V. Katavić performed research, analyzed data, and critically revised the manuscript.

A. Marušić designed research and critically revised the manuscript.

D. Grčević designed research, performed research, and critically revised the manuscript.

N. Kovačić designed research, performed research, analyzed data, wrote, and critically revised the manuscript.

All authors have read and approved the final version of the manuscript.

References

1. Feldmann, M., Brennan, F.M., Maini, R.N. (1996) Rheumatoid arthritis. Cell85, 307–10
2. McInnes, I.B., Schett, G. (2007) Cytokines in the pathogenesis of rheumatoid arthritis. Nat Rev Immunol7, 429–442
3. Furuzawa-Carballeda, J., Vargas-Rojas, M.I., Cabral, A.R. (2007) Autoimmune inflammation from the Th17 perspective. Autoimmun Rev6, 169–175
4. Lotito, A.P.N., Silva, C.A.A., Mello, S.B.V. (2007) Interleukin-18 in chronic joint diseases. Autoimmun Rev6, 253–256
5. Malemud, C.J. (2011) Dysfunctional immune-mediated inflammation in rheumatoid arthritis dictates that development of anti-rheumatic disease drugs target multiple intracellular signaling pathways. Antiinflamm Antiallergy Agents Med Chem10, 78–84
6. Malemud, C.J. (2009) Recent advances in neutralizing the IL-6 pathway in arthritis. Open Access Rheumatol1, 133–150
7. Hartgring, S.A.Y., Bijlsma, J.W.J., Lafeber, F.P.J.G., van Roon, J.A.G. (2006) Interleukin-7 induced immunopathology in arthritis. Ann Rheum Dis65, 69–74
8. Petrovic-Rackov, L., Pejnovic, N. (2006) Clinical significance of IL-18, IL-15, IL-12 and TNF-alpha measurement in rheumatoid arthritis. Clin Rheumatol25, 448–452
9. Collison, L.W., Workman, C.J., Kuo, T.T., Boyd, K., Wang, Y., Vignali, K.M., Cross, R., Sehy, D., Blumberg, R.S., Vignali, D.A. (2007) The inhibitory cytokine IL-35 contributes to regulatory T-cell function. Nature450, 566–569
10. Bottini, N., Firestein, G.S. (2012) Duality of fibroblast-like synoviocytes in RA: passive responders and imprinted aggressors. Nat Rev Rheumatol9, 24–33
11. Walsh, N.C., Gravallese, E.M. (2010) Bone remodeling in rheumatic disease: a question of balance. Immunol Rev233, 301–312
12. Schett, G. (2009) Osteoimmunology in rheumatic diseases. Arthritis Res Ther11, 210
13. Šućur, A., Katavić, V., Kelava, T., Jajić, Z., Kovačić, N., Grčević, D. (2014) Induction of osteoclast progenitors in inflammatory conditions: Key to bone destruction in arthritis. Int Orthop38, 1893–1903
14. Boyce, B.F., Xing, L. (2008) Functions of RANKL/RANK/OPG in bone modeling and remodeling. Arch Biochem and Biophys473, 139–146
15. Li, X., Makarov, S.S. (2006) An essential role of NF-kappaB in the “tumor-like” phenotype of arthritic synoviocytes. Proc Natl Acad Sci U S A103, 17432–17437
16. Lazić, E., Jelušić, M., Grčević, D., Marušić, A., Kovačić, N. (2012) Osteoblastogenesis from synovial fluid-derived cells is related to the type and severity of juvenile idiopathic arthritis. Arthritis Res Ther14,

R139

17. Malemud, C.J. (2013) Intracellular Signaling Pathways in Rheumatoid Arthritis. J Clin Cell Immunol4, 160
18. Diarra, D., Stolina, M., Polzer, K., Zwerina, J., Ominsky, M.S., Dwyer, D., Korb, A., Smolen, J., Hoffmann, M., Scheinecker, C., van der Heide, D., Landewe, R., Lacey, D., Richards, W.G., Schett, G. (2007) Dickkopf-1 is a master regulator of joint remodeling. Nat Med1, 156–163
19. Aggarwal, B.B. (2003) Signalling pathways of the TNF superfamily: a double-edged sword. Nat Rev Immunol3, 745–756
20. Askenasy, N., Yolcu, E.S., Yaniv, I., Shirwan, H. (2005) Induction of tolerance using Fas ligand: A double-edged immunomodulator. Blood105, 1396–1404
21. Kovacić, N., Lukić, I.K., Grcević, D., Katavić, V., Croucher, P., Marusić, A. (2007) The Fas/Fas ligand system inhibits differentiation of murine osteoblasts but has a limited role in osteoblast and osteoclast apoptosis. J Immunol178, 3379–3389
22. Nakamura, T., Imai, Y., Matsumoto, T., Sato, S., Takeuchi, K., Igarashi, K., Harada, Y., Azuma, Y., Krust, A., Yamamoto, Y., Nishina, H., Takeda, S., Takayanagi, H., Metzger, D., Kanno, J., Takaoka, K., Martin, T.J., Chambon, P., Kato, S. (2007) Estrogen prevents bone loss via estrogen receptor alpha and induction of Fas ligand in osteoclasts. Cell130, 811–823
23. Katavić, V., Lukić, I.K., Kovačić, N., Grcević, D., Lorenzo, J. A., Marusić, A. (2003) Increased bone mass is a part of the generalized lymphoproliferative disorder phenotype in the mouse. J Immunol170, 1540–1547
24. Krum, S.A., Miranda-Carboni, G.A., Hauschka, P.V., Carroll, J.S., Lane, T.F., Freedman, L.P., Brown, M. (2008) Estrogen protects bone by inducing Fas ligand in osteoblasts to regulate osteoclast survival. EMBO J27, 535–545
25. Wu, X., McKenna, M.A., Feng, X.U., Nagy, T.R., McDonald, J.M. (2003) Osteoclast apoptosis: the role of Fas in vivo and in vitro. Endocrinology144, 5545–5555
26. Calmon-Hamaty, F., Audo, R., Combe, B., Morel, J., Hahne, M. (2015) Targeting the Fas/FasL system in Rheumatoid Arthritis therapy: Promising or risky? Cytokine75, 228–233
27. Peng, S.L. (2006) Fas (CD95)-related apoptosis and rheumatoid arthritis. Rheumatology (Oxford)45, 26–30
28. Fujisawa, K., Asahara, H., Okamoto, K., Aono, H., Hasunuma, T., Kobata, T., Iwakura, Y., Yonehara, S., Sumida, T., Nishioka, K. (1996) Therapeutic effect of the anti-Fas antibody on arthritis in HTLV-I tax transgenic mice. J Clin Invest 98, 271–278
29. Zhang, H., Yang, Y., Horton, J. L., Samoilova, E.B., Judge, T.A., Turka, L.A., Wilson, J.M., Chen, Y.

(1997) Amelioration of collagen-induced arthritis by CD95 (Apo-1/Fas)-ligand gene transfer. J Clin Invest100, 1951–1957

30. Kim, S.H., Kim, S., Oligino, T.J., Robbins, P.D. (2002) Effective treatment of established mouse collagen-induced arthritis by systemic administration of dendritic cells genetically modified to express FasL. Mol Ther6, 584–590
31. Schedel, J., Gay, R.E., Kuenzler, P., Seemayer, C., Simmen, B., Michel, B.A., Gay, S. (2002) FLICE-inhibitory protein expression in synovial fibroblasts and at sites of cartilage and bone erosion in rheumatoid arthritis. Arthritis Rheum46, 1512–1518
32. García, S., Liz, M., Gómez-Reino, J. J., Conde, C. (2010) Akt activity protects rheumatoid synovial fibroblasts from Fas-induced apoptosis by inhibition of Bid cleavage. Arthritis Res Ther12, R33
33. Tu-Rapp, H., Hammermüller, A., Mix, E., Kreutzer, H.J., Goerlich, R., Köhler, H., Nizze, H., Thiesen, H.J., Ibrahim, S.M. (2004) A proinflammatory role for Fas in joints of mice with collagen-induced arthritis. Arthritis Res Ther6, R404-414
34. Ma, Y., Liu, H., Tu-Rapp, H., Thiesen, H.J., Ibrahim, S.M., Cole, S.M., Pope, R.M. (2004) Fas ligation on macrophages enhances IL-1R1-Toll-like receptor 4 signaling and promotes chronic inflammation. Nat Immunol5, 380–387
35. Huang, Q.Q., Birkett, R., Koessler, R.E., Cuda, C.M., Haines, G.K. 3rd, Jin, J.P., Perlman, H., Pope, R.M. (2014) Fas signaling in macrophages promotes chronicity in K/BxN serum-induced arthritis. Arthritis Rheumatol66, 68–77
36. Adachi, M., Suematsu, S., Kondo, T., Ogasawara, J., Tanaka, T., Yoshida, N., Nagata, S. (1995) Targeted mutation in the Fas gene causes hyperplasia in peripheral lymphoid organs and liver. Nat Genet11, 294–300
37. Odobasic, D., Leech, M. T., Xue, J. R., Holdsworth, S.R. (2008) Distinct in vivo roles of CD80 and CD86 in the effector T-cell responses inducing antigen-induced arthritis. Immunology124, 503–513
38. Ikić Matijašević, M., Flegar, D., Kovačić, N., Katavić, V., Kelava, T., Šućur, A., Ivčević, S., Cvija, H., Lazić Mosler, E., Kalajzić, I., Marušić, A., Grčević, D. (2016) Increased chemotaxis and activity of circulatory myeloid progenitor cells may contribute to enhanced osteoclastogenesis and bone loss in the C57BL/6 mouse model of collagen-induced arthritis. Clin Exp Immunol186, 321–335
39. Grčević, D., Sironi, M., Valentino, S., Deban, L., Cvija, H., Inforzato, A., Kovačić, N., Katavić, V., Kelava, T., Kalajzić, I., Mantovani, A., Bottazzi, B. (2018) The Long Pentraxin 3 Plays a Role in Bone Turnover and Repair. Front Immunol9, 417
40. Krause, U., Seckinger, A., Gregory, C.A. (2011) Chapter 17, Mesenchymal Stem Cell Assays and Applications (Vemuri, M. C. et al., eds.), Methods in Molecular Biology, Springer, Berlin, Germany

41. Conover, W.J. (1999) Practical nonparametric statistics, third edition (Wiley, B., and O'Sullivan, M., eds), John Wiley & Sons, New York
42. Chan, C.K.F., Seo, E.Y., Chen, J.Y., Lo, D., McArdle, A., Sinha, R., Tevlin, R., Seita, J., Vincent-Tompkins, J., Wearda, T., Lu, W.J., Senarath-Yapa, K., Chung, M.T., Marecic, O., Tran, M., Yan, K.S., Upton, R., Walmsley, G.G., Lee, A.S., Sahoo, D., Kuo, C.J., Weissman, I.L., Longaker, M.T. (2015) Identification and specification of the mouse skeletal stem cell. Cell. 160, 285–298
43. Kovacic, N., Grcevic, D., Katavic, V., Lukic, I.K., Grubisic, V., Mihovilovic, K., Cvija, H., Croucher, P. I., Marusic, A. (2010) Fas receptor is required for estrogen deficiency-induced bone loss in mice. Lab Invest90, 402–413
44. Paquet, J., Goebel1, J., Delaunay, C., Pinzano, A., Grossin, L.,Cournil-Henrionnet, C., Gillet, P., Netter, P., Jouzeau, J., Moulin, D. (2012) Cytokines profiling by multiplex analysis in experimental arthritis: which pathophysiological relevance for articular versus systemic mediators? Arthritis Research & Therapy14, R60
45. Ostendorf, B., Scherer, A., Specker, C., Mödder, U., Schneider, M. (2003) Jaccoud's arthropathy in systemic lupus erythematosus: Differentiation of deforming and erosive patterns by magnetic resonance imaging. Arthritis Rheum48, 157–165
46. Adachi, M., Suematsu, S., Suda, T., Watanabe, D., Fukuyama, H., Ogasawara, J., Tanaka, T., Yoshida, N., Nagata, S. (1996) Enhanced and accelerated lymphoproliferation in Fas-null mice. Proc Natl Acad Sci U S A93, 2131-2136
47. Park, H., Jung, Y.K., Park, O.J., Lee, Y.J., Choi, J.Y., Choi, Y. (2005) Interaction of Fas ligand and Fas expressed on osteoclast precursors increases osteoclastogenesis. J Immunol175, 7193–7201
48. Parijs, L.V. (1998) Homeostasis and self-tolerance in the immune system: turning lymphocytes off. Science280, 243–248
49. Daniel, P.T., Krammer, P.H. (1994) Activation induces sensitivity toward APO-1 (CD95)-mediated apoptosis in human B cells. J Immunol152, 5624–5632
50. Jagger, A.L., Evans, H.G., Walter, G.J., Gullick, N.J., Menon, B., Ballantine, L.E., Gracie, A., Magerus-Chatinet, A., Tiemessen, M.M., Geissmann, F., Rieux-Laucat, F., Taams, L.S. (2012) FAS/FAS-L dependent killing of activated human monocytes and macrophages by CD4+CD25- responder T cells, but not CD4+CD25+ regulatory T cells. J Autoimmun38, 29–38
51. Amouzegar, A., Mittal, S.K., Sahu, A., Sahu, S.K., Chauhan, S.K. (2017) Mesenchymal Stem Cells Modulate Differentiation of Myeloid Progenitor Cells During Inflammation. Stem Cells35, 1532–1541

Figure legends

Figure 1. Arthritis score in wild-type (wt) and Fas-deficient (Fas –/–) mice.

Wild-type and Fas –/– mice were sacrificed on day 10 following intraarticular (i.a.) injection of methylated bovine serum albumin (mBSA). **(A)** Representative images of 6 μm Goldner-trichrome (upper panels) and toluidine-blue (lower panels)-stained mid-frontal femoral sections of wt and Fas –/– mice, i.a. injected with mBSA (AIA) or PBS (ctrl). **(B)** Transverse diameter of both knees was measured post-sacrifice, after the skin removal, using a vernier scale/caliper. **(C)** Total histology score measured in the right knee, in wt and Fas -/- mice i.a. injected with mBSA (AIA) or PBS (ctrl). Scoring was performed in a blinded fashion according to synovial thickenning (black arrows), exudate in joint space (red arrow), cartilage degradation (green arrowhead), and subchondral bone damage (yellow arrows), according to the 3 point scale. **(D)** Percentage of non-degraded cartilage thickness in total cartilage thickness, in wt and Fas –/– mice i.a. injected with mBSA (AIA) or PBS (ctrl), measured by histomorphometry. **(E)** Separate histology scores in wt and Fas –/– mice intra-articularly (i.a.) injected with mBSA (AIA) or PBS (ctrl). Data are from a representative of three repeated experiments, where both knees were measured three times taking mean value for each knee for statistical analysis (N (B6 ctrl)=18, N (B6 AIA)=16, N (Fas ctrl)=12, and N (Fas AIA)=14). Right knee was used for histology scoring and cartilage thickness measurements (N (B6 ctrl)=9, N (B6 AIA)=7, N (Fas ctrl)=6, and N (Fas AIA)=7, excluding one slide in B6 AIA group due to inappropriate orientation). Markers represent individual values, horizontal line and error bars are mean±SD (B) or median±IQR (C-E); B, influence of genotype (g) and arthritis (a) on knee diameter, statistical significance of interaction between both factors, p(gxa) is marked on plos, two-way ANOVA; C-E, Kruskal-Wallis test); bars, 150 μm.

Figure 2. Histomorphometry and micro-CT analysis of distal femoral epiphyseal trabecular bone of wild-type (wt) and Fas-deficient (Fas –/–) mice on day 10 of antigen-induced arthritis.

The following variables were analyzed in distal femoral epiphyses from wt and Fas –/– mice intraarticularly (i.a.) injected with mBSA (AIA) or PBS (ctrl): trabecular bone volume (BV/TV, %), trabecular number (Tb.N, mm^{-2}), trabecular thickness (Tb.Th, μm), and trabecular separation (Tb.Sp, mm). **(A)** Histomorphometry analysis of the trabecular bone in the distal femoral epiphyses, **(B)** representative 3D models of distal femora, from micro-CT reconstruction images, and **(C)** quantitative micro-CT analysis of the trabecular bone in the distal femoral epiphyses. Histomorphometry data are from a representative of three repeated experiments (N (B6 ctrl)=9, N (B6 AIA)=7, N (Fas ctrl)=6, and N (Fas AIA)=7), and micro-CT are cumulative data from three representative experiments (N (B6 ctrl)=24, N (B6 AIA)=27, N (Fas ctrl)=18, and N (Fas AIA)=22). Markers represent individual values, horizontal lines and error bars are mean±SD. Influence of genotype (g) and arthritis

(a) on each bone-related variable was assessed by two-way ANOVA, statistical significance of interaction between both factors, p(gxa) is marked on plots. Arrows, bone erosions.

Figure 3. Expression of Fas on hematopoetic and non hematopoietic lineage cells on day 10 of antigen-induced arthritis.

(A) Cells from the synovial compartment (Syn) and spleen (SPL) from control non immunised mice (ctrl-NI), immunised mice injected intra-articularly (i.a.) with PBS (ctrl-IM) and with mBSA (AIA) were harvested, and synovial single cell suspensions were stained with anti-mouse CD95-AF488 or corresponding isotype control, anti-mouse CD45-APC, TER119-PE, and CD31-PECy7 antibodies, whereas spleen cells were stained with anti-CD95-AF488 or corresponding isotype control, CD11b-PE, Gr-1-PECy7, B220-APC, and CD3-APCCy7 antibodies. Data are from a representative of two repeated experiments, both knees from each mouse were harvested and pooled for flow cytometry analysis (N (B6 NI)=5, N (B6 ctrl)=6, N (B6 AIA)=7). Mean fluorescence intensities (MFI) for each population are shown as individual values (markers), horizontal lines and bars are mean±SD, * $p<0.05$ vs. ctrl-NI mice, ** $p<0.05$ vs. ctrl-IM mice ($p<0.05$, ANOVA and Student-Newman-Keuls post-hoc test). **(B)** Expression of Fas, FasL, TNF, IL-1β, IL-6, IL-10, RANKL, and OPG mRNA in total knee joint tissue from control non immunised (ctrl-NI), and immunised wild-type (wt) and Fas-deficient mice (Fas –/–) mice injected intra-articularly (i.a.) with mBSA (AIA). Both knees from each mouse were harvested and pooled for RNA extraction (N (B6 NI)=5, N (B6 AIA)=5, N (Fas NI)=6, and N (Fas AIA)=7). Markers represent individual gene expression values in each mouse, normalized to gene expression of β actin, horizontal lines and error bars are median±IQR; * $p<0.05$ vs. ctrl-NI mice, ** $p<0.05$ vs. wt mice (Kruskal-Wallis test).

Figure 4. Osteoblastogenesis and proportions of synovial non hematopoietic cells in wild-type (wt) and Fas-deficient (Fas-/-) mice with antigen-induced arthritis.

(A) Synovia-derived osteoblast colonies from immunised wild-type (wt) and Fas-deficient (Fas –/–) mice injected intra-articularly (i.a.) with PBS (ctrl) and mBSA (AIA) on day 14 of cell culture, stained for AP (red) and with methylene blue (MB). Data are from one of three repeated experiments, where cells were isolated from 6-8 mice per group and pooled for culture. **(B)** Semiquantitave data are mean±SD of AP+ surface per cm^2 triplicate wells of 6-well culture plate (N=3). Influence of genotype (g) and arthritis (a) on AP+ surface was assessed by two-way ANOVA, statistical significance of interaction between both factors, p(gxa) is marked on plot. **(C)** Expression of osteoblast genes, runt-related transcription factor 2 (*runx2*) collagen type I, α2 chain (*Col Iα2*), osteocalcin (*bglap*), and osteoprotegerin (*OPG*), during synovia-derived osteoblast differentiation. The data are from two repeated experiments where cells were isolated from 6-8 mice per group and pooled for culture. RNA was harvested from 3 pooled wells of 24-well culture plate. Relative quantity of a gene in each experiment was normalized to relative quantity of β actin, and average quantity of each gene on day 0.

Horizontal lines and bars are mean±SD of both experiments (N=2). Influence of experimental group (gr) and culture day (d) on expression of each gene was assessed by two-way ANOVA, statistical significance of interaction between both factors, p(gr×d), and significant influence of culture culture day, p(d) is marked on plots. For flow cytometry analysis, single cell suspensions were stained with anti-mouse CD90.2-FITC, CD200–PE, CD105-PECy7, CD45-APC, TER119-APC, CD31-APC and CD51-biotin/streptavidin-APCeF780 antibodies. Dead cells were excluded by binding of 7-AAD. Proportions of $CD45^-TER119^-CD31^-CD51^+$ (non hematopoietic bone and cartilage progenitor) cells were determined amongst single live cells. Proportion of $CD200^+CD105^-$, CD200–, and CD200–$CD105^+CD90.2^+$ cells was determined amongst $CD45^-TER119^-CD31^-CD51^+$ cells. **(D)** Dot plots showing $CD200^+$ and CD200– cells in the concatenated samples from a representative experiment. **(E)** Upper panels, proportions of $CD45^-TER119^-CD31^-CD51^+$ cells in total live synovial cells, and $CD200^+CD105^-$, CD200–, and CD200–$CD105^+CD90.2^+$ in $CD45^-TER119^-CD31^-CD51^+$cells, shown as individual values (markers). Data are from a representative of three repeated experiments, where left knees were used for cell dissociation and flow cytometry. Horizontal lines and bars are mean±SD, N (B6 ctrl)=9, N (B6 AIA)=8, N (Fas ctrl)=6, and N (Fas AIA)=7. Influence of genotype (g) and arthritis (a) on proportions of osteoprogenitor populations was assessed by two-way ANOVA, statistical significance of interaction between both factors, p(gxa), and significant influence of genotype, p(g), is marked on plots.

Figure 5. Expression of Fas in synovial mesenchymal cells. (A) Representative histograms and **(B)** proportions of live cells expressing hematopoietic and mesenchymal markers on day 7 (upper panels) and 14 (lower panels) in osteoblastogenic cultures of sorted $CD45^-CD31^-TER119^-CD51^+$ cells. Red histograms, stained cells, black histograms, non-stained cells. Cultured cells were harvested on culture days 7 and 14, and labeled with anti-mouse CD95-FITC or the isotype control, anti-mouse CD45-APC, CD31-APC, TER119-APC, CD51-APCeF780, CD200–PE, and CD105-PECy7. Experiments were repeated three times and data are mean of quadriplicate wells of the representative experiment. Statistical significance is marked on plots (d7 vs. d14, t-test) **(C)** Representative histograms and **(D)** proportions of live $CD200^+$, and CD200– cells labeled with anti-mouse CD95-FITC, on culture days 7 (upper panels) and 14 (lower panels) in osteoblastogenic cultures of sorted $CD45^-CD31^-TER119^-CD51^+$ cells. Cultured cells were labeled with anti-mouse CD95-FITC, and proportion of $CD95^+$ cells (red histograms) was determined according to the signal of corresponding isotype control (black histograms). Experiments were repeated three times and data are mean of duplicate wells of the representative experiment. Statistical significance is marked on plots (d7 vs. d 14, t-test)**. (E)** Expression of Fas mRNA in osteoblastogenic cultures of sorted mesenchymal progenitors ($CD45^-CD31^-TER119^-CD51^+$). Data are mean±SD of Fas mRNA realative expression in three repeated experiments (N=3), normalized to quantity on day 7, statistical significance is marked on plot (d7 vs. d 14, t-test). **(F)** Osteoblast colonies from sorted mesenchymal progenitors ($CD45^-CD31^-TER119^-CD51^+$) on day 7 and 14 of cell culture, stained for AP, with

alizarin red (AR), and total colonies stained with methylene blue (MB). **(G)** Semi-quantitative assessment of AP+ red surface area, and absorbance (A) of acetic acid-extracted AR on day 7 and 14 of cell culture, both measured in four wells of 6-well culture plate. Data are mean±SD of four replicates, statistical significance is marked on plot (d7 vs. d 14, t-test).

Figure 6. Susceptibility of synovial mesenchymal cells to Fas-mediated apoptosis. (A) Representative dot plots showing proportions of apoptotic (lower right quadrant) and dead (upper right quadrant) cells, determined by labeling with annexin V-FITC and 7-AAD, and **(B)** proportion of $CD200^+$ cells amongst single cells, on day 7 (upper panels) and 14 (lower panels) in osteoblastogenic cultures from sorted synovial mesenchymal progenitors treated with 1 μg/mL anti-mouse CD95 antibody, or 1 μg/mL of isotype control antibody and 1 μg/mL protein G, or only 1 μg/mL protein G (NT), on culture days 6 and 13, and harvested after 16-18 hours. Experiments were repeated two times, in duplicate and triplicate wells which were pooled for analysis, and data are from representative experiment.

Figure 1

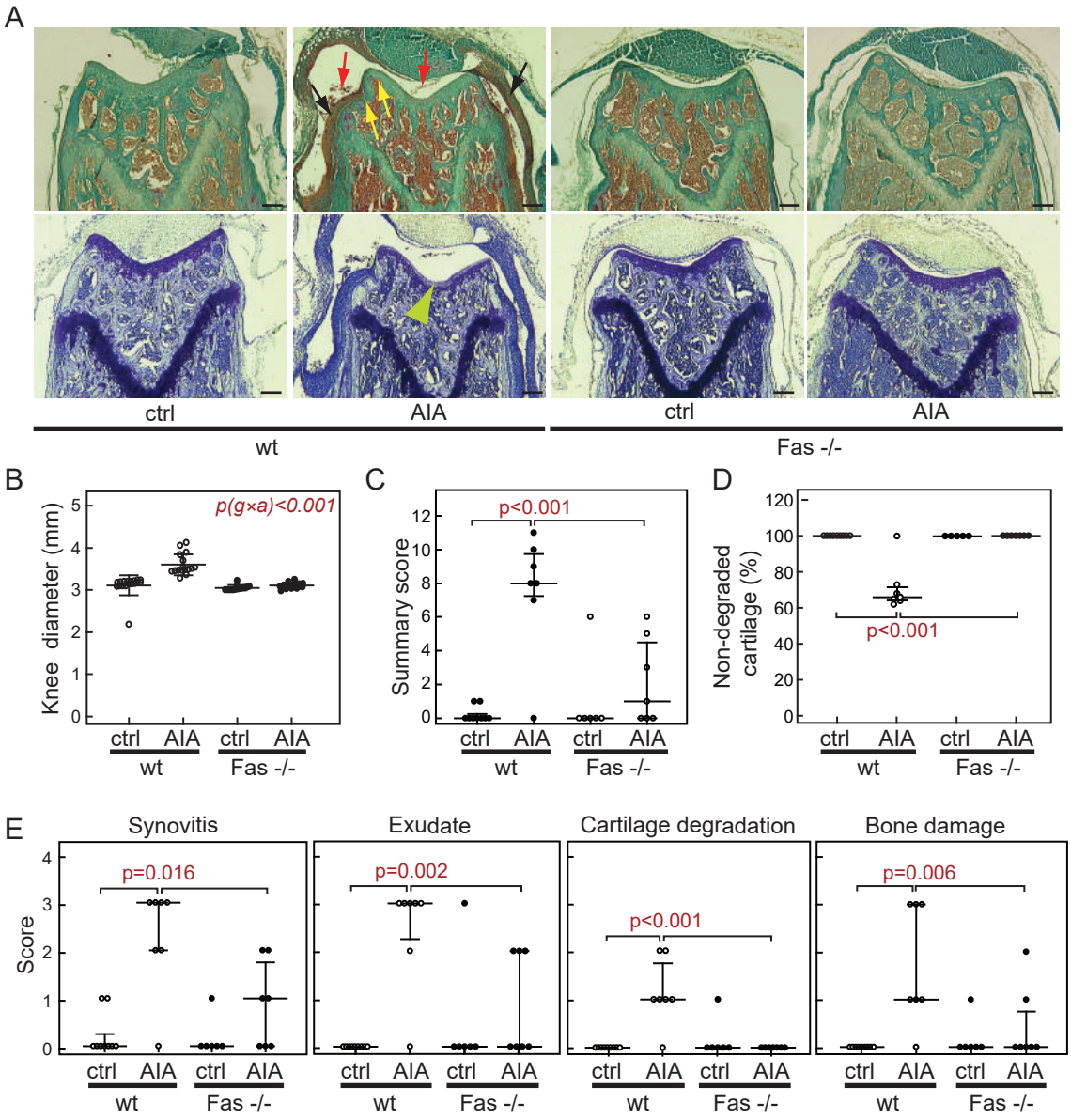
A
ctrl
AIA
ctrl
AIA
wt
Fas -/-
B
Knee diameter (mm)
p(g×a)<0.001
ctrl AIA ctrl AIA
wt
Fas -/-
C
Summary score
p<0.001
ctrl AIA ctrl AIA
wt
Fas -/-
D
Non-degraded cartilage (%)
p<0.001
ctrl AIA ctrl AIA
wt
Fas -/-
E
Synovitis
Exudate
Cartilage degradation
Bone damage
Score
p=0.016
p=0.002
p<0.001
p=0.006
ctrl AIA ctrl AIA
wt
Fas -/-

Figure 2

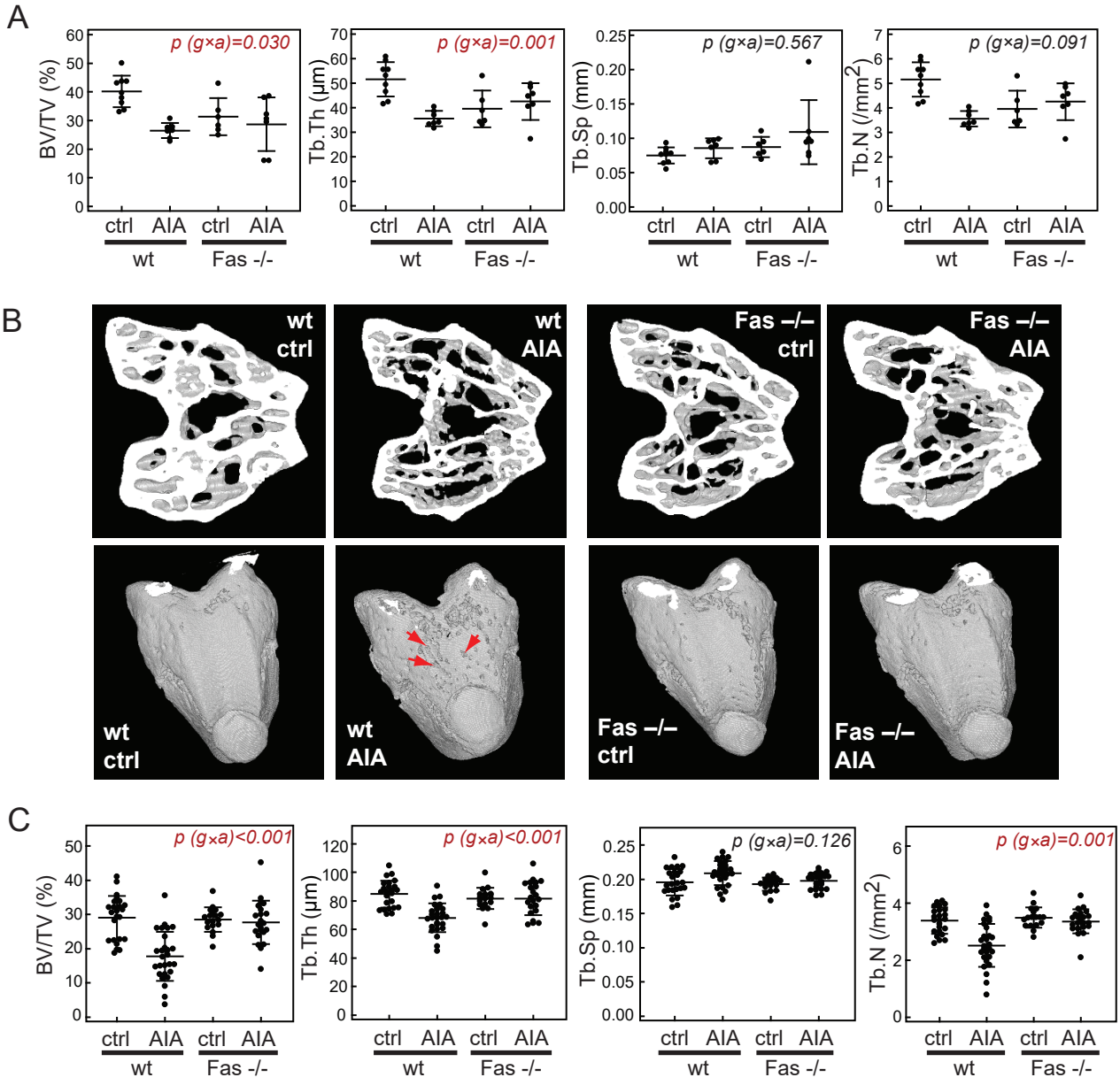
A
BV/TV (%)
p (g×a)=0.030
Tb.Th (µm)
p (g×a)=0.001
Tb.Sp (mm)
p (g×a)=0.567
Tb.N (/mm2)
p (g×a)=0.091
ctrl AIA ctrl AIA
wt Fas -/-
B
wt ctrl
wt AIA
Fas –/– ctrl
Fas –/– AIA
C
BV/TV (%)
p (g×a)<0.001
Tb.Th (µm)
p (g×a)<0.001
Tb.Sp (mm)
p (g×a)=0.126
Tb.N (/mm2)
p (g×a)=0.001
ctrl AIA ctrl AIA
wt Fas -/-

Figure 3

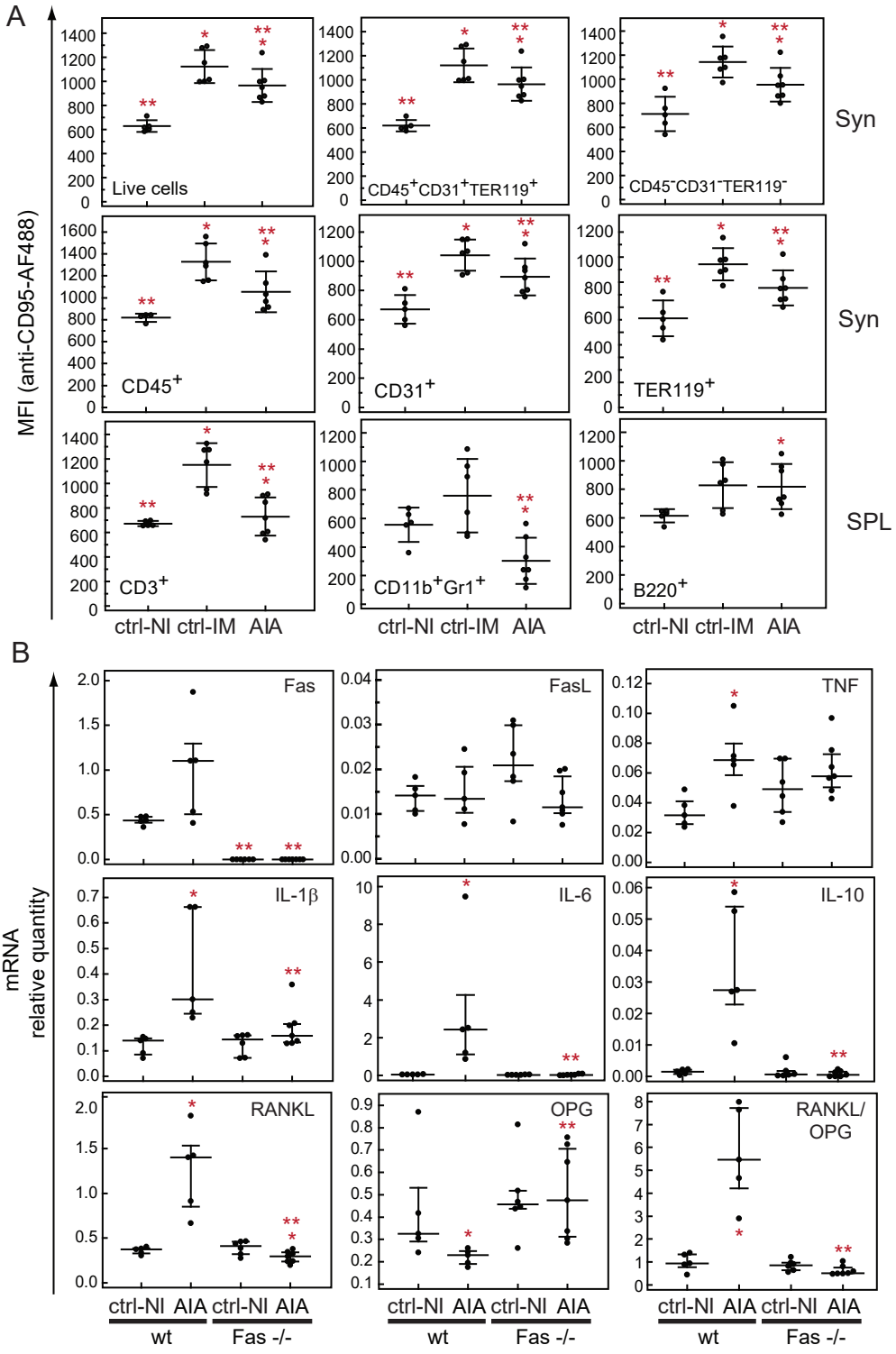
A
MFI (anti-CD95-AF488)
Live cells
CD45+CD31+TER119+
CD45-CD31-TER119-
Syn
CD45+
CD31+
TER119+
Syn
CD3+
CD11b+Gr1+
B220+
SPL
ctrl-NI ctrl-IM AIA
B
mRNA relative quantity
Fas
FasL
TNF
IL-1β
IL-6
IL-10
RANKL
OPG
RANKL/ OPG
ctrl-NI AIA ctrl-NI AIA
wt
Fas -/-

Figure 4

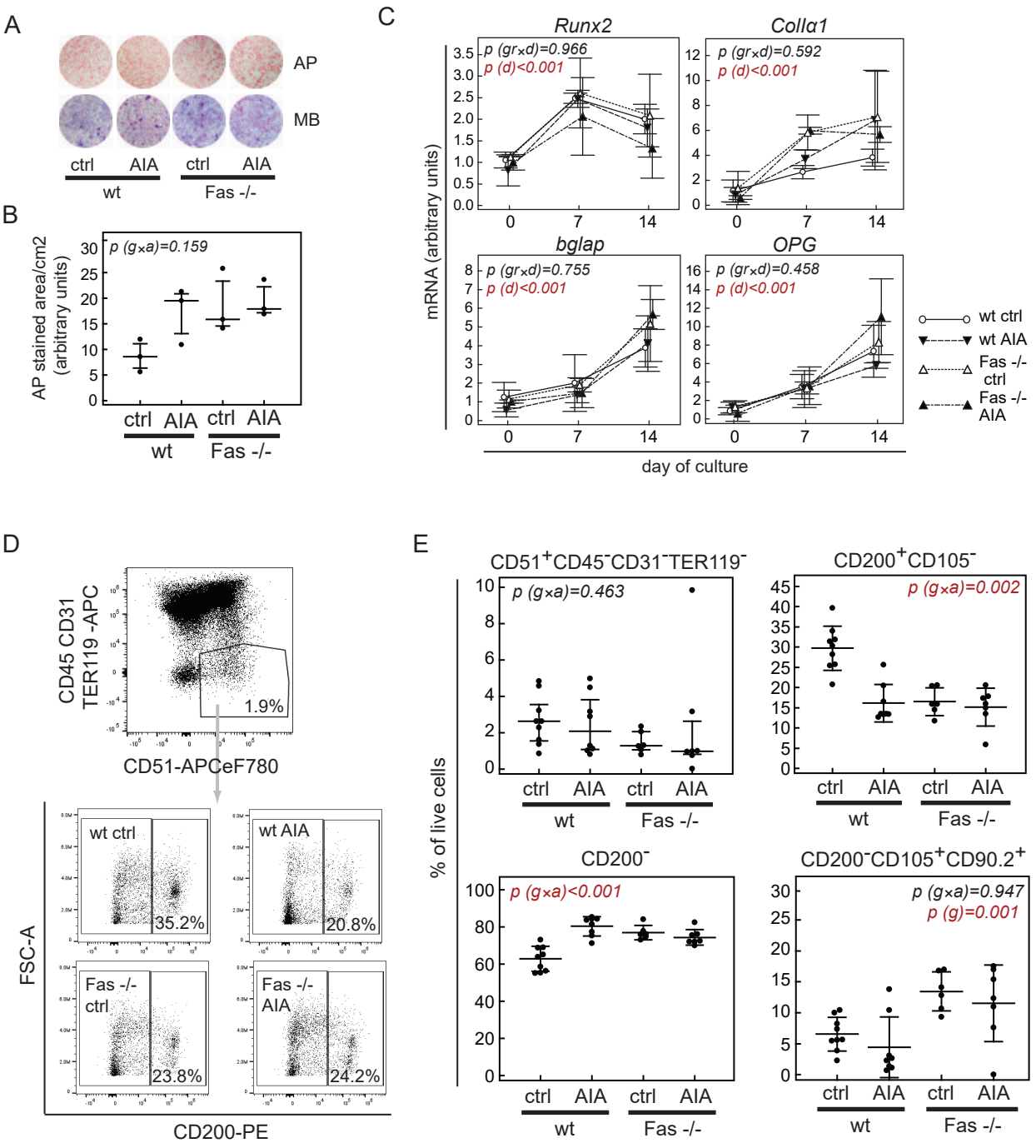
A
AP
MB
ctrl
AIA
ctrl
AIA
wt
Fas -/-
B
AP stained area/cm2 (arbitrary units)
p (g×a)=0.159
ctrl
AIA
ctrl
AIA
wt
Fas -/-
C
Runx2
p (gr×d)=0.966
p (d)<0.001
Collα1
p (gr×d)=0.592
p (d)<0.001
bglap
p (gr×d)=0.755
p (d)<0.001
OPG
p (gr×d)=0.458
p (d)<0.001
mRNA (arbitrary units)
day of culture
wt ctrl
wt AIA
Fas -/- ctrl
Fas -/- AIA
D
CD45 CD31 TER119 -APC
1.9%
CD51-APCeF780
wt ctrl
35.2%
wt AIA
20.8%
Fas -/- ctrl
23.8%
Fas -/- AIA
24.2%
FSC-A
CD200-PE
E
CD51+CD45-CD31-TER119-
p (g×a)=0.463
CD200+CD105-
p (g×a)=0.002
% of live cells
CD200-
p (g×a)<0.001
CD200-CD105+CD90.2+
p (g×a)=0.947
p (g)=0.001
ctrl
AIA
ctrl
AIA
wt
Fas -/-

Figure 5

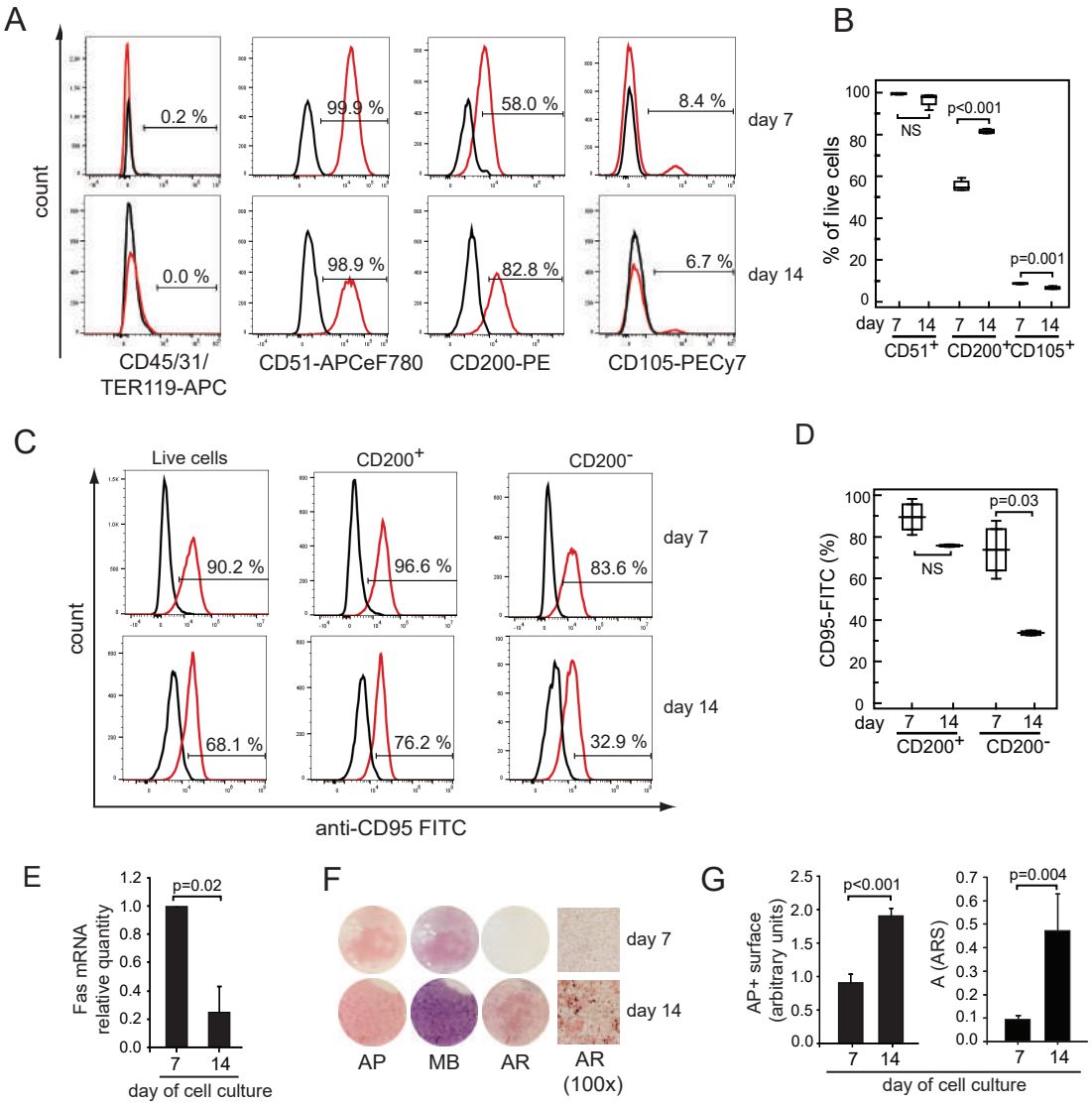
A
count
0.2 %
99.9 %
58.0 %
8.4 %
day 7
0.0 %
98.9 %
82.8 %
6.7 %
day 14
CD45/31/
TER119-APC
CD51-APCeF780
CD200-PE
CD105-PECy7
B
% of live cells
p<0.001
NS
p=0.001
day
7 14 7 14 7 14
CD51+ CD200+ CD105+
C
Live cells
CD200+
CD200-
90.2 %
96.6 %
83.6 %
day 7
68.1 %
76.2 %
32.9 %
day 14
count
anti-CD95 FITC
D
CD95-FITC (%)
p=0.03
NS
day
7 14 7 14
CD200+ CD200-
E
Fas mRNA
relative quantity
p=0.02
7 14
day of cell culture
F
day 7
day 14
AP MB AR
AR
(100x)
G
AP+ surface
(arbitrary units)
p<0.001
A (ARS)
p=0.004
7 14 7 14
day of cell culture

Figure 6

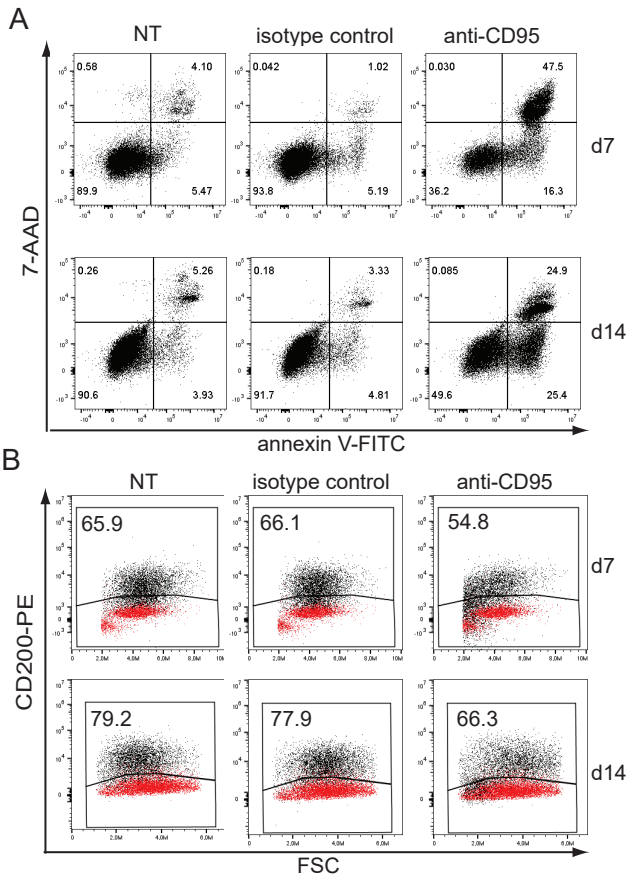
A
NT
isotype control
anti-CD95
0.58
4.10
89.9
5.47
0.042
1.02
93.8
5.19
0.030
47.5
36.2
16.3
d7
0.26
5.26
90.6
3.93
0.18
3.33
91.7
4.81
0.085
24.9
49.6
25.4
d14
7-AAD
annexin V-FITC
B
NT
isotype control
anti-CD95
65.9
66.1
54.8
d7
79.2
77.9
66.3
d14
CD200-PE
FSC